CARBON 49 (2011) 5246–5252

Available at www.sciencedirect.com

SciVerse ScienceDirect

journal homepage: www.elsevier.com/locate/carbon

The photoinduced charge transfer mechanism in aligned and unaligned carbon nanotubes

Gianluca Galimberti [a], *Stefania Pagliara* [a,*], *Stefano Ponzoni* [a], *Stefano Dal Conte* [b], *Federico Cilento* [c], *Gabriele Ferrini* [a], *Stephan Hofmann* [d], *Muhammad Arshad* [e,h,i], *Cinzia Cepek* [f], *Fulvio Parmigiani* [g]

[a] *Dipartimento di Matematica e Fisica, Università Cattolica del Sacro Cuore, I-25121 Brescia, Italy*
[b] *Dipartimento di Fisica, Università di Pavia, I-27100 Pavia, Italy*
[c] *Dipartimento di Fisica, Università di Trieste and Laboratorio Nazionale TASC, AREA Science Park, Basovizza, Trieste I-34012, Italy*
[d] *Department of Engineering, University of Cambridge, Cambridge CB3 0FA, UK*
[e] *ICTP, Strada Costiera 11, I-34151 Trieste, Italy*
[f] *Istituto Officina dei Materiali - CNR, Laboratorio TASC, Area Science Park, Basovizza, I-34149 Trieste, Italy*
[g] *Dipartimento di Fisica, Università di Trieste and Sincrotrone Trieste, I-34012 Basovizza, Trieste, Italy*
[h] *Zernike Institute for Advanced Materials, University of Groningen, The Netherlands*
[i] *National centre for Physics Quaid-i-Azam University Islamabad, Pakistan*

ARTICLE INFO

Article history:
Received 4 April 2011
Accepted 21 July 2011
Available online 28 July 2011

ABSTRACT

Using time-resolved reflectivity measurements on unaligned and aligned bundled single-wall carbon nanotubes with a pump energy of 1.55 eV, quasi-resonant with the second *Van Hove* singularity of semiconducting tubes, a positive sign of the transient reflectivity is detected in unaligned nanotubes. In contrast a negative sign is detected in aligned nanotubes. This discovery addresses a long-standing question showing that in unaligned nanotubes the stronger intertube interactions favor the formation of short-lived free charge carriers in semiconducting tubes. A detailed analysis of the transient reflectivity spectral response shows that the free carriers in the photo-excited state of semiconducting tubes move towards metallic tubes in about 400 fs.

1. Introduction

In these last years a significant effort has been addressed to identify the carbon nanotube (CNT) orientation most suitable for CNT-based electronic devices. The performance of these devices, ranging from field effect transistors to nano-photovoltaic systems, strongly depend on non equilibrium carrier transport and on charge transfer mechanisms from semiconducting to metallic nanotubes [1–4]. Therefore, a correct understanding of intertube interactions and charge transfer mechanisms is a *key issue* for a significant advance of the technology of CNT-based devices.

Here, by performing time resolved reflectivity measurements on aligned and unaligned single wall carbon nanotube (SWCNT) bundles we unveil the physical mechanism at the basis of the charge transfer from semiconducting to metallic tube.

A large number of studies have shown that at equilibrium [5–7], the intertube interactions in SWNT bundles are weak and similar to the coupling between adjacent graphene planes in 3D crystalline graphite or the interball coupling found in solid C_{60}. This weak intertube coupling is dominated by the van der Waals interactions with a nonzero covalent bonds contribution. These behavior have a significant

* *Corresponding author:* Fax: +39 030 2406 742.
E-mail address: pagliara@dmf.unicatt.it (S. Pagliara).
0008-6223/$ - see front matter
doi:10.1016/j.carbon.2011.07.042

influence on the vibrational [5,6,8–11] and electronic states of carbon nanotubes [12–14]. Nonetheless, the effect of the intertube interactions in bundled CNTs, relevant to charge transfer mechanisms, remains unclear.

A number of theoretical studies have been performed to address the effects of intertube interactions in bundled nanotubes. These studies suggest that the dominating intertube van der Waals interactions, while promoting the nanotube bundling, have the effect of energy shifting and broadening the optical transitions. In particular, the broadening of the absorption spectral features, in bundled nanotubes, originates from the intertube electronic properties perpendicular to the tube axis. Moreover, the curvature of the nanotube wall in CNTs induces a downshift of the conduction bands by enhancing the σ–π hybridization [6,15,16].

Although these mechanisms are well understood, the absence of a strong luminescence in CNT bundles remains unclear. This is a key question concerning the charge transfer processes since it has been argued that the non-radiative channel, quenching the radiative channel (fluorescence), can originate from possible charge transfer from the semiconducting to the metallic tubes [15]. Nevertheless, this is still an open question and optical spectroscopies in the time domain, with a suitable time resolution, might reveal the changes of the optical properties induced by nonradiative mechanisms [17–20]. Recently, this kind of experiments have been performed on CNTs with a well defined chirality. However, making CNTs with a defined structure and with intertube interactions not affected from other atomic species (contaminants, surfactants or molecule) still remains a major challenge [21,22]. In this framework, in order to highlight the dependence of the charge transfer channel on the bare intertube interactions, time-resolved reflectivity measurements in the femtosecond timescale have been carried out on aligned and unaligned SWCNT bundles with different chirality, grown in the same experimental conditions [23].

The experiments have been performed by using a conventional one-color pump–probe set-up (pump and probe both at 1.55 eV), along with a novel pump-probe set-up in which the probe is a broadband white light pulse (supercontinuum) [24]. By using the supercontinuum pulse as a probe, it is possible to achieve spectral resolution: this allows to detect in the frequency domain the relaxation dynamics of the carriers excited through a resonant absorption transition into the conduction band. By setting the pump frequency quasi-resonant with the second *Van Hove* singularity of the carbon compounds a positive sign of the transient reflectivity is detected in unaligned nanotubes, whereas a negative transient reflectivity is detected in aligned nanotubes. This important difference demonstrates that in unaligned nanotubes the stronger intertube interactions favor the formation of short-living free charge carriers in semiconducting tubes that decay through a charge transfer nonradiative process toward the metallic tubes. A detailed analysis of the transient reflectivity spectral response shows that the free carriers in the photo-excited state of semiconducting tube transfer to the metallic tubes in about 400 fs.

The important results emerging from our findings are: (i) bundling and unalignement induce strong intertube interactions yielding a free-electron mobility of the excited carriers in semiconducting tube; (ii) the photoinduced charge delocalization favours the charge transfer from semiconducting to metallic tube.

2. Experimental

2.1. Sample preparation

Aligned and unaligned CNT bundles (Fig. 1a, Fig. 1b) were synthesized in the Analytical Division of the TASC-IOM-CNR laboratory, where the catalyst depositions and Chemical Vapor Deposition (CVD) processes are performed in an ultra high vacuum experimental apparatus (base pressure $<1\times10^{-10}$ mbar). In this apparatus it is possible to control the chemical state of the catalyst (before and after the growth) via X-ray photoemission spectroscopy (XPS) and to monitor all the CVD parameters (i.e. precursor gas purity, pressure and pressure gradient, sample temperature, gas fluxes, etc.).

Pure aligned and unaligned SWNT bundles were grown via CVD technique by using the same CVD parameters [23]. Only the precursor gas pressure has been changed in order to obtain aligned and unaligned bundles. SWCNTs were characterized by microRaman and SEM measurements (see Supplementary Data).

2.2. Laser system

Time-resolved reflectivity (TR) measurements have been performed with two laser systems, to investigate different pump fluence regimes. An amplified 1 kHz Ti:Sapphire laser system, producing 150 fs, 1.55 eV light pulses, permits to excite the samples with pump fluences in the range 10–100 mJ/cm^2, whereas with a cavity-dumped Ti:Sapphire oscillator, producing 120 fs, 1.55 eV light pulses, the samples have been excited with pump fluences ranging from 0.1 to 0.8 mJ/cm^2.

The incidence angle of the laser pump is about 5° with respect to the sample normal direction.

This laser system is also equipped with a supercontinuum generation unit [24], to collect TR spectra with both time and frequency resolution, with an energy range from 1.1 to 2.0 eV. (see Supplementary Data).

3. Results and discussion

Because of the one-dimensional nature of the electronic bands, the density of states of SWCNT exhibits a series of characteristic Van Hove singularities (VHSs) detectable in the near IR and visible spectral regions (Fig. 1a).

Fig. 1b shows a representative reflectivity spectrum, collected on unaligned SWNT bundles. Four structures located at about 0.8 eV (TA), 1.35 eV (TB), 2.2 eV(TC) and 3.1 eV (TD) are clearly detected. The features TA,TB and TD are assigned to the inhomogeneously broadened interband optical transitions from the valence subbands to their respective conduction subbands in semiconducting SWCNTs as schematically shown in Fig. 1a. Instead, the band TC is assigned to an interband transition in metallic SWCNTs [17,18].

When the photon pump energy is resonant with a VHS, a transient photobleaching is usually expected in the one-color

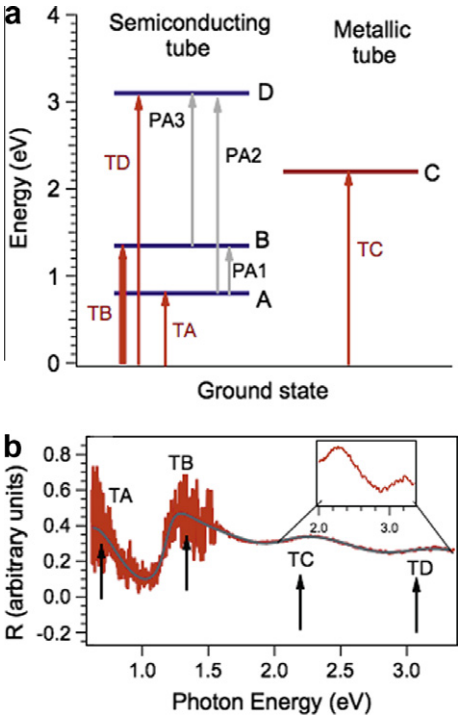

Fig. 1 – (a) Schematic electronic structure of both semiconducting and metallic unaligned bundled SWNTs. The energy positions of the bands (A, B, C and D) are estimated by the reflectivity spectrum reported in (b). The arrows TA, TB, TC and TD indicate the transitions from the ground state to unoccupied states. PA1, PA2 and PA3 refer to photoabsorption processes induced by the laser pump nearly resonant with TB transition.

time-resolved optical spectroscopies. Absorption of the pump pulse excites electrons into conduction band, creating holes in the valence band. Until these carriers relax, transient filling effects on the final states are observed. For the photobleaching effect, the transient signal is positive in trasmittivity and negative in reflectivity (such as in the absorption) [18–20,25].

Fig. 2 shows the one-color transient reflectivity on unaligned SWCNT bundles (Fig. 2b) together with the spectrum acquired on aligned SWCNT bundles (Fig. 2a).

While the negative TR signal on aligned SWCNTs reveals the photobleaching process in agreement with literature [18–20,26], the positive TR signal on unaligned SWCNTs is the fingerprint of a new relaxation channel that increases the reflectivity.

We attribute the positive TR signal to a free-electron like character of the carriers excited in the B band of semiconducting tubes. The TR negative sign of the substrate including the catalyst nanoparticles suggests that the contribution of the substrate (inset in Fig. 2b) is negligible. Moreover, the different orientation of the laser polarization with respect to the CNT axis in the unaligned and aligned bundles can not justify a different sign in the transient optical response.

At this pump photon energy, the VHS optical transitions are excited only with an electric field parallel to the tube axis. Due to the near-normal incidence of the laser pump, we expect strong excitation mainly in the unaligned bundles, where the laser polarization, in a statistical sense, can be found parallel to the tube axis [27]. However, also in the vertically aligned bundles the excitation of the VHS transitions cannot be excluded even at near normal incidence, considering the imperfect alignement of the CNTs that prevents them to be perfectly normal to the incident electric field of the pump beam. As a consequence, the laser pump excites the same VHS transition in both samples, the only difference being the excitation intensity. In agreement with literature [27–29], due to the dependence of absorption coefficient on the relative CNT – electric field orientation, we conclude that only the density of the photoexcited carriers and not the sign of the transient reflectivity is affected by the excitation of the VHS transitions.

The positive TR sign can be rationalized considering that in the aligned SWCNTs the intertube interactions is comparable with the van der Waals interactions among the graphene layers in graphite, whereas in unaligned SWCNT the intertube interactions are changed by both the curvature and the spatial anisotropy. In particular, the modified intertube interactions induce an overlap between the π-bands of adjacent tubes by allowing the delocalization of the electrons photoexcited in the VHS. Usually, the presence of VHSs or, alternatively, of the strongly bound excitons inhibit the free-carrier mobility yielding to a localization of charge carriers on a length scale of ≈100 nm [30]. The modified intertube interactions in the unaligned bundles, on the contrary, delocalize the carriers excited in these bands, inhibiting the photobleaching and favouring the free-electron mobility.

The delocalized charge optical response is expected to behave as a Drude electron gas. In this case the imaginary part of the dielectric function can be written as [31]:

$$\varepsilon_2(\omega) = \frac{\omega_p^2 \tau}{\omega(1+\omega^2\tau^2)} \quad (1)$$

where $\omega_p^2 = (Ne^2)/(\varepsilon_0 m)$ is the plasma frequency, N the carrier density, e and m the charge and the mass of the electron, ε_0 the vacuum dielectric constant.

For an ideal free-electron metal, the reflectivity approaches unity below the plasma frequency. Above the plasma frequency, the metal is transparent and the reflectivity decreases rapidly with increasing frequency.

When free-electron carriers are created by the laser pump, the Drude-like behaviour of the carriers enhances the reflectivity. Therefore, the transient reflectivity, which is the reflectivity signal of the probe modified by the presence of the laser pump, is positive and it can be directly related to the CNT orientation (aligned or unaligned SWCNT bundles).

To further support this finding, TR measurements on films with different CNT density, length and substrates have been performed. The TR positive signal shows no dependence on these sample characteristics (see Supplementary Data). Moreover, to rule out spurious effects such as nonlinear processes and sample damage the experiments have been repeated varying the laser fluence from 10 to 80 mJ/cm^2 and from 0.1 to 0.8 mJ/cm^2 (shown in Fig. 3a and b). In Fig. 3c and d the dependence of the maximum of the TR signal on the pump laser fluence is shown. For pump fluence ranging from 0.1 mJ/cm^2 to 0.8 mJ/cm^2 (Fig. 3d), TR signal linearly increases with

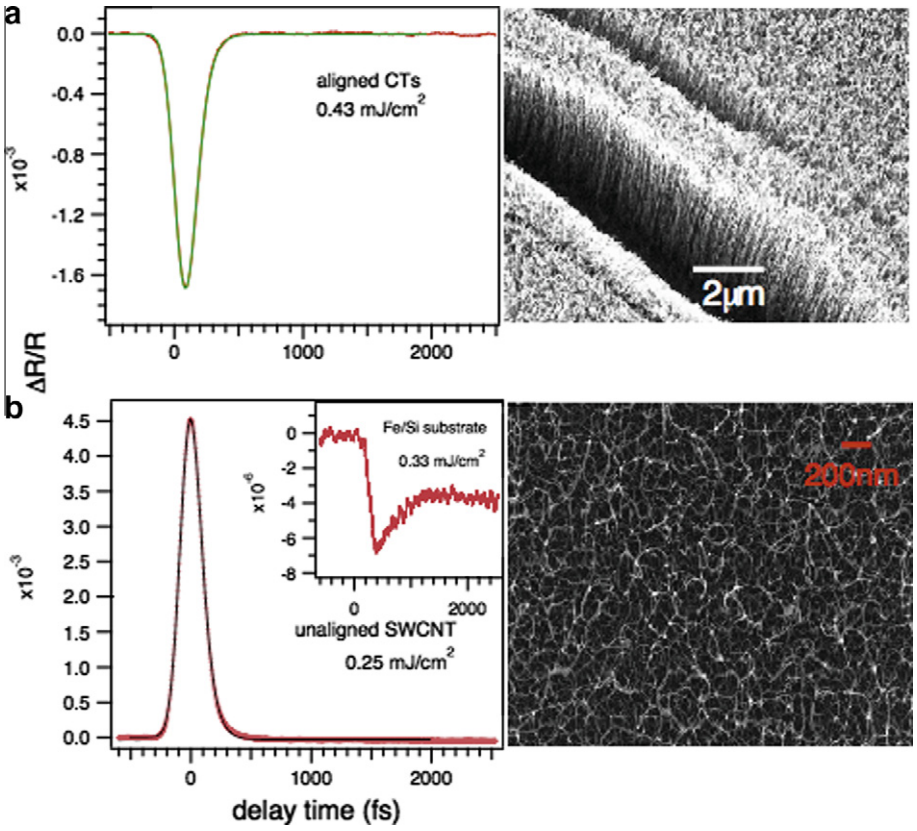

Fig. 2 – One-color ($h\nu$ = 1.55 eV, fluence of 0.2 mJ/cm^2) transient reflectivity spectra collected on both aligned (a) and unaligned (b) SWCNT. The TR spectrum of the substrate is also reported (inset in (b)) in order to exclude its contribution on the TR signal of unaligned bundles. The spectra of unaligned and aligned SWCNTs are well fitted with one exponential curve convoluted with a gaussian (representing the laser pulsewidth). The SEM images are also reported.

fluence, whereas the saturation effect takes place (Fig. 3c) above 40 mJ/cm^2. To estimate the carrier density excited (N(E)) in the π^* band the following formula can be used [32]:

$$\int_0^{\infty} N(E)dE = \frac{(1-R)F\alpha}{h\nu} \quad (2)$$

where $h\nu$ is 1.5 eV, the reflectivity $R = 0.4$ and the absorption coefficient $\alpha = 2\times10^5$ cm^{-1}. Therefore at a laser fluence $F = 40$ mJ/cm^2, the initial photo-carrier density is 20×10^{21} cm^{-3}. This value is comparable (including non-linear optical processes that become important at this high pump fluence) with the carriers density from 0 to 1 eV (6.5×10^{21} cm^{-3}) observed in graphite [32]. This result proves that at the pump intensity used in this experiment and at a photon frequency quasi-resonant with the second VHS a very high density of carriers can be excited in the π^* band of the semiconducting tube.

To obtain information about the dynamics of the excited-state carriers, the spectra reported in Fig. 3a and b are fitted with exponential curves convoluted with a Gaussian representing the laser pulsewidth. The TR spectra of both aligned and unaligned SWCNT bundles are well fitted by one exponential curve with a decay time (≈100 fs) comparable with the laser pulsewidth (Fig. 2a and b). Moreover, the dependence of the relaxation time on the fluence (Fig. 3e and f) excludes radiative recombination processes [33].

This result is in agreement with the dynamics of the bundles reported in literature [19,29] and it can be justified considering that in CNTs the carrier dynamics strongly depend on the excited state. In particular, when electrons are excited in the first VHS of the semiconducting tubes (A) the lifetime is ≈1 ps [19], whereas in the second (B) the lifetime is ≈130 fs. Meanwhile, the luminescence from isolated CNT has a longer lifetime (≈30 ps) than that on unaligned bundles. This can be explained considering that the carriers excited into the second VHS relax very rapidly to the band gap of the semiconducting tube (intraband scattering). Then in isolated nanotubes the electron and the hole recombine across the band gap, whereas in bundled nanotubes the tunneling into nearby metallic tubes or into semiconducting tubes with a smaller band gap turns off the luminescence. The excited carriers in the metallic tubes, as shown in time-resolved photoemission experiments [17,34,35], lose their energy rapidly, therefore quenching the luminescence of CNT bundles efficiently [15,17,34,35]. In this experiment, the presence of a fast relaxation channel on unaligned SWCNT bundles confirms that electrons are excited in the second VHS. This behavior is compatible with a free character of the excited carriers in the semiconducting tubes that favors the charge transfer towards metallic tubes and semiconducting tubes with smaller energy gap. The mechanisms so far described can be understood in more details looking at the optical

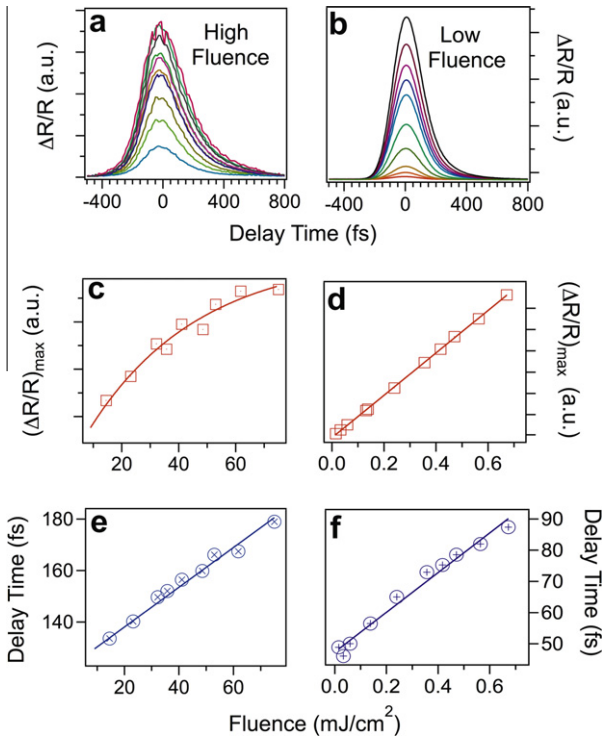

Fig. 3 – (a and b) One-color transient reflectivity spectra collected on unaligned SWCNT bundles by changing the pump laser fluence. The spectra are collected at different fluence regimes: high fluence (from 10 to 80 mJ/cm^2) and low fluence (from 0.1 to 0.8 mJ/cm^2). (c and d) Pump fluence dependence of the maximum of the transient reflectivity spectra and (e and f) of the relaxation time, estimated by fitting the spectra with one exponential decay curve convoluted with a gaussian. The solid curves represent the best fit of these data with a linear (d, e and f) and an exponential curve (c).

response of photoexcited SWNT in both the time and frequency domains.

In these experiments the pump photon energy is 1.55 eV, whereas the probe covers an energy range from 1.1 to 2 eV (Fig. 4a). In SWCNT, a photobleaching process is usually correlated with different photoabsorption channels [18]. In particular, carriers excited in the B band rapidly decay on A giving rise to PA1, PA2 and PA3 photoabsorption processes, where carriers are photoexcited from A to B (PA1), from A to D (PA2) and from B to D (PA3) (see Fig. 1a). By considering the reflectivity spectrum collected on bundled SWCNT sample (Fig. 1b), the photoabsorption channels could appear at 0.6 eV (PA1), 2.3 eV (PA2) and 1.7 eV (PA3).

The 3-dimensional (3D) TR spectrum is shown in Fig. 4a together with different extracted line profiles at fixed delay times (Fig. 4b and c) or photon energies (Fig. 4d and e). The broad red line at about $h\nu = 1.55$ eV (Fig. 4a) covers the laser pump scattered by the sample. The image profile at delay time $\tau = 0$ fs (Fig. 4b) shows two positive features. The first, broadband and centered at 1.4 eV, is the TB transition; its positive signal confirms the free-electron character of the excited carriers discussed in one-color TR at 1.55 eV. This band appears structured due to the noise in the measurement.

The second positive feature at 1.65 eV is ascribed to the PA3 photoabsorption process. Electrons are excited by the probe from the B band to the D band in the pulsewidth. This picture is confirmed by the lack of relaxation processes before the photoabsorption (PA3 appears at $\tau = 0$ fs in Fig. 4b). To analyze the relaxation dynamics of the PA3 channel, the line profile at $h\nu = 1.65$ eV is shown (Fig. 4d). From the fitting with exponential curves, the PA3 decay results very fast and after a pump–probe delay of about 400 fs, a negative TR signal with a long decay time is observed. In the 3D spectrum, a dark-purple zone corresponding to a negative TR signal is evident around the point $h\nu = 1.95$ eV, $\tau = 400$ fs (Fig. 4e). This negative zone extends up to 2 eV and appears after $\tau = 400$ fs. In the reflectivity spectrum of Fig. 1b, the feature at about 2 eV has been ascribed to the TC transition in the metallic tubes. As the pump photon energy at 1.55 eV is unable to excite any transition in the metallic tube, the presence of this photobleaching channel, which implies a filling of the C band, is the evidence of a charge transfer from the semiconducting to the metallic tube.

These observations can be interpreted considering that the pump laser excites a population in the B band of the semiconducting SWCNTs. Some of the delocalized carriers are excited by the same pump pulse in the D band. By calculating the area of the TR spectrum at $\tau = 0$ fs (Fig. 4b), the intensity of the PA3 photoabsorption process can be estimated resulting comparable with that of free-carriers excited in the B band. Because of their mobility, the carriers transfer from the semiconducting to the metallic tube within 400 fs, giving rise to a photobleaching of the TR when the probe photon energy is nearly resonant with the TC transition. The lack of the B and C band photobleaching in the reflectivity spectrum reported in literature [18] confirms that the two mechanisms are mutually exclusive and that only the free-electron behaviour of the excited carriers permits to switch on the semiconducting-metallic charge transfer.

The slow relaxation dynamics of the C photobleaching (about 2 ps, see image profile at $h\nu = 1.95$ eV of Fig. 4e) agrees with the dynamics of the photobleaching channels reported in literature on SWCNTs [20].

To perform a quantitative study of the TR spectrum at $\tau = 0$ fs, a differential dielectric function model has been fitted to the time-resolved-reflectivity data, $\Delta R/R = (R_{ex}(\varepsilon_{ex}) - R_{eq}(\varepsilon_{eq}))/R_{eq}(\varepsilon_{eq})$, where R_{ex}, ε_{ex}, R_{eq}, ε_{eq} are the excited and equilibrium reflectivity and dielectric function, respectively. The ε_{eq} has been calculated by fitting R_{eq} (Fig. 1b) with a sum of Lorentz oscillators which represent the transitions TA, TB, TC, TD.

According to the differential dielectric function model [36], for reproducing the transient reflectivity spectrum, it occurs to modify the fitting parameters of the Lorentz oscillators or to add new oscillators. In our case, to properly fit the differential spectrum $\Delta R/R$ (Fig. 4b), we need to add one Drude and one Lorentz oscillator, the first to take into account the free-electron mobility of the photoexcited carriers in the B band, and the second to reproduce the PA3 photoabsorption at 1.7 eV. The presence of solitonic structures in the supercontinuum affects the fitting accuracy of the line profile at $\tau = 0$ fs with the differential model. However it is possible to extrapolate a value for the plasma frequency in the Drude model (Eq. (1)) of

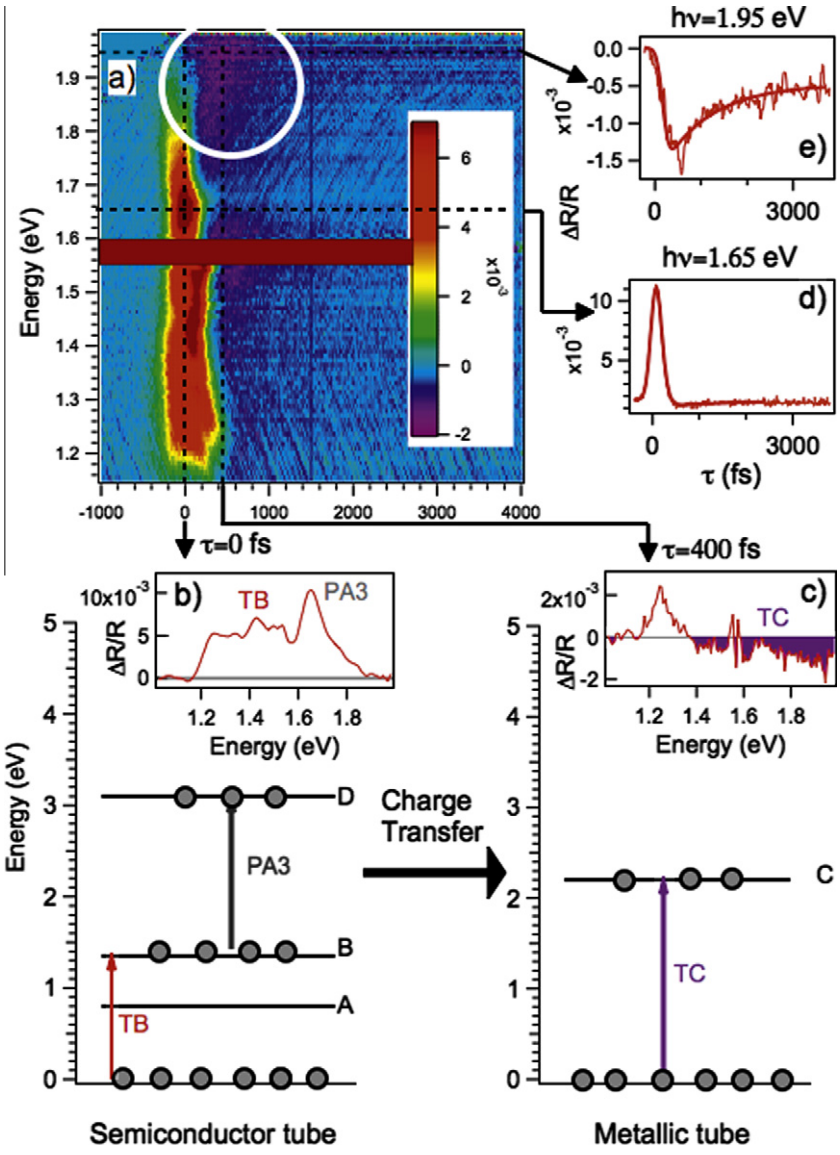

Fig. 4 – (a) 3D image of the time resolved reflectivity spectrum collected on unaligned SWCNT bundles by using the supercontinuum probe and a $h\nu$ = 1.55 eV pump. On the bottom a scheme of the charge transfer. At τ = 0 the carriers are excited in the B band of the semiconducting tubes by the laser pulse. Some of the carriers are excited by the same pulse into the D band (PA3 transition in (b)). After 400 fs (c), carriers in the excited-states of semiconducting tube move towards the metallic tube and a negative TR signal due to TC transition appears in the probe spectrum. On the right, image profiles extracted at photon energies of the probe corresponding to PA3 (d) and TC transitions (e).

4×10^{15} sec^{-1} (2.5 eV), that corresponds to a carrier density of 4×10^{21} cm^{-3}. This value, compared with the carrier density excited by the laser pump (2×10^{20} cm^{-3} for a pump fluence of 0.2 mJ/cm^2 (Eq. 2)), confirms the delocalized character of the carriers excited in the B band of semiconducting tubes.

4. Conclusion

Time-resolved reflectivity measurements demonstrate that intertube interactions in bundled unaligned SWCNTs induce a free-electron character to the photoexcited carriers favoring a charge transfer from semiconducting to metallic tube. This finding paves the road to new and important technologies closely connected to the intra- and inter-tube conductivity.

Acknowledgment

The authors would like to thank Dr. Lidia Armelao and Dr. Pietro Galinetto for reflectivity and Raman measurements. Moreover, we acknowledge Dr. Claudio Giannetti for the discussions on the supercontinuum experimental setup. C.C. thanks the FP7 Technotubes (grant agreement: CP-IP 228579-1) for supporting this work.

Appendix A. Supplementary data

Supplementary data associated with this article can be found, in the online version, at doi:10.1016/j.carbon.2011.07.042.

REFERENCES

[1] Avouris P, Chen Z, Perebeinos V. Carbon-based electronics. Nat Nanotechol 2007;2(10):605–15.
[2] Jorio A, Dresselhaus G, Dresselhaus MS. Carbon Nanotubes, Advanced Topics in the Synthesis, Structure, Properties and Applications. Springer; 2008.
[3] Bockrath M, Cobden DH, McEuen PL, Chopra NG, Zettl A, Thess A, et al. Single-electron transport in ropes of carbon nanotubes. Science 1997;275(5308):1922–5.
[4] Derycke V, Martel R, Appenzeller J, Avouris Ph. Carbon nanotube inter- and intramolecular logic gates. Nano Lett 2001;1(9):453–6.
[5] Rao AM, Chen J, Richter E, Schlecht U, Eklund PC, Haddon RC, et al. Effect of van derWaals Interactions on the Raman Modes in SingleWalled Carbon Nanotubes. Phys. Rev. Lett. 2001;86(17):3895–8.
[6] Reich S, Maultzsch J, Thomsen C, Ordejón P. Tight-binding description of graphene. Phys Rev B 2002;66(3):035412–35416.
[7] Borondics F, Kamaras K, Nikolou M, Tanner DB, Chen ZH, Rinzler AG. Charge dynamics in transparent single-wall nanotube films from optical transmission measurements. Phys Rev B 2006;74(4):045431–45436.
[8] Venkateswaran UD, Rao AM, Richter E, Menon M, Rinzler A, Smalley RE, et al. Probing the single-wall carbon nanotube bundle: Raman scattering under high pressure. Phys Rev B 1999;59(16):10928–34.
[9] Kahn D, Lu JP. Probing the single-wall carbon nanotube bundle: Raman scattering under high pressure. Phys Rev B 1999;60(9):6535–40.
[10] Henrard L, Hernandez E, Bernier P, Rubio A. Van der Waals interaction in nanotube bundles: Consequences on vibrational modes. Phys Rev B 1999;60(12):R8521–4.
[11] Kurti J, Kresse G, Kuzmany H. First-principles calculations of the radial breathing mode of single-wall carbon nanotubes. Phys Rev B 1998;58(14):R8869–72.
[12] Delany P, Hyoung JC, Ihm J, Louie SG, Cohen ML. Broken symmetry and pseudogaps in ropes of carbon nanotubes. Nature (London) 1998;391(6666):466–8.
[13] Kwon YK, Saito S, Tomanek D. Effect of intertube coupling on the electronic structure of carbon nanotube ropes. Phys Rev B 1998;58(20):R13314–7.
[14] Alvarez L, Righi A, Guillard T, Rols S, Anglaret E, Laplaze D, et al. Resonant Raman study of the structure and electronic properties of single-wall carbon nanotubes. Chem Phys Lett 2000;316(1-2):186–90.
[15] Reich S, Dworzak M, Hoffmann A, Thomsen C, Strano MS. Excited-state carrier lifetime in single-walled carbon nanotubes. Phys Rev B 2005;71(3):033402–33405.
[16] Blase X, Benedict LX, Shirley EL, Louie SG. Hybridization Effects and Metallicity in Small Radius carbon Nanotubes. Phys Rev Lett 1994;72(12):1878–81.
[17] Hertel T, Fasel R, Moos G. Charge-carrier dynamics in single-wall carbon nanotube bundles: a time-domain study. Appl Phys A 2002;75(4):449–65.
[18] Korovyanko OJ, Sheng C-X, Vardeny ZV, Dalton AB, Baughman RH. Ultrafast Spectroscopy of Excitons in Single-Walled Carbon Nanotubes. Phys Rev Lett 2004;92(1):017403–6.
[19] Lauret J-S, Voisin C, Cassabois G, Delalande C, Roussignol Ph, Jost O, et al. Ultrafast Carrier Dynamics in Single-Wall Carbon Nanotubes. Phys Rev Lett 2003;90(5):057404–7.
[20] Manzoni C, Gambetta A, Menna E, Meneghetti M, Lanzani G, Cerullo G. Intersubband Exciton Relaxation Dynamics in Single-Walled Carbon Nanotubes. Phys Rev Lett 2005;94(20):207401–4.
[21] Luer L, Crochet J, Hertel T, Cerullo G, Lanzani G. Ultrafast excitation energy transfer in small semiconducting carbon nanotube aggregates. ACSNano 2010;4(7):4265–73.
[22] Zheng M, Semke ED. Enrichment of single chirality carbon nanotubes. JACS 2007;129(19):6084–5.
[23] Hofmann S, Sharma R, Ducati C, Du G, Mattevi C, Cepek C, et al. In situ observation of catalyst dynamics during surface-bound carbon nanotube nucleation. Nano Lett 2007;7(3):602–8.
[24] Cilento F, Giannetti C, Ferrini G, Dal Conte S, Sala T, Coslovich G, et al. Ultrafast insulator-to-metal phase transition as a switch to measure the spectrogram of a supercontinuum light pulse. Appl Phys Lett 2010;96(2):021102–4.
[25] Ma Y-Z, Valkunas L, Dexheimer SL, Bachilo SM, Fleming GR. Femtosecond Spectroscopy of Optical Excitations in Single-Walled Carbon Nanotubes: Evidence for Exciton-Exciton Annihilation. Phys Rev Lett 2005;94(15):157402–5.
[26] Kato K, Ishioka K, Kitajima M, Tang J, Saito R, Petek H. Coherent phonon anisotropy in aligned single-walled carbon nanotubes. Nano Lett 2008;8(10):3102–8.
[27] Murakami Y, Einarsson E, Edamura T, Maruyama S. Polarization Dependence of the Optical Absorption of Single-Walled Carbon Nanotubes. Phys Rev Lett 2005;94(8):087402–5.
[28] Hashimoto Y, Murakami Y, Maruyama S, Kono J. Anisotropic decay dynamics of photoexcited aligned carbon nanotube bundles. Phys Rev B 2007;75(24):245408–12.
[29] Reich S, Thomsen C, Maultzsch J. Carbon Nanotubes: Basic Concepts and Physical Properties. WILEY-VCH Verlag GmbH & Co. KGaA; 2004.
[30] Perfetti L, Kampfrath T, Schapper F, Hagen A, Hertel T, Aguirre CM, et al. Ultrafast Dynamics of Delocalized and Localized Electrons in Carbon Nanotubes. Phys Rev Lett 2006;96(2):027401–4.
[31] Wooten F. Optical properties of solids. Academic Press; 1972.
[32] Seibert K, Cho GC, Kutt W, Kurz H, Reitze DH, Dadap JI, et al. Femto second carrier dynamics in graphite. Phys Rev B 1990;42(5):2842–51.
[33] Ostojic GN, Zaric S, Kono J, Strano MS, Moore VC, Hauge RH, et al. Interband Recombination Dynamics in Resonantly Excited Single-Walled Carbon Nanotubes. Phys Rev Lett 2004;92(11):117402–5.
[34] Hertel T, Moos G. Electron-Phonon Interaction in Single-Wall Carbon Nanotubes: A Time- Domain Study. Phys Rev Lett 2000;84(21):5002–5.
[35] Hagen A, Moos G, Talalaev V. Hertel, T. Electronic structure and dynamics of optically excited single-wall carbon nanotubes. Appl Phys A 2004;78(8):1137–45.
[36] Basov DN, Averitt RD, van der Marel D, Dressel M, Haule K. Electrodynamics of correlated electron materials. Rev. Mod. Phys. 2011; 83(2): 471-541. See, in particular, pag. 475. More information on the differential dielectric function model is available on the website http://optics.unige.ch/alexey/reffit.html